A LETTERS JOURNAL EXPLORING THE FRONTIERS OF PHYSICS

July 2009

EPL, **87** (2009) 10007
doi: 10.1209/0295-5075/87/10007

www.epljournal.org

SPR-based infrared detection of aqueous and gaseous media with silicon substrate

R. JHA[1(a)(b)] and A. K. SHARMA[2(a)(c)]

[1] *Mediterranean Technology Park - Carrer de la Coruna, 13, 08860, Castelldefels, Barcelona, Spain*
[2] *Jacob Ruisdaellaan 3, 5581 JK, Waalre, The Netherlands*

received 26 April 2009; accepted in final form 18 June 2009
published online 24 July 2009

PACS 07.07.Df – Sensors (chemical, optical, electrical, movement gas, etc.); remote sensing

Abstract – A high-accuracy surface plasmon resonance (SPR) sensor with silicon substrate and Al-Au bimetal is proposed for aqueous and gaseous detection in infrared (IR) with a single probe. Angular interrogation method is used for SPR excitation using infrared source in the Kretschmann-Reather configuration. Sensor's performance is analyzed in terms of intrinsic sensitivity (IS) that includes the width and shift of SPR curve for given refractive index of sensing medium. In a broadband IR range of 1200 nm (700 nm–1900 nm), the IS of the Al-Au bimetal-based silicon sensor is almost 350% more as compared with an Au-based one, which is the most widely used SPR active metal. The oxidation problem of the Al-based SPR sensor has been addressed. The physical explanation related to the results has been provided. Further, the performance of the proposed sensor design is better for gaseous sensing as compared to liquid sensing.

In the last two decades, the surface plasmon resonance (SPR)-based detection mechanism has secured a very important place among the several sensing techniques due to its better performance and reliable procedure. Since its first application in gas sensing [1], SPR has been widely used for different sensing applications [2–4] due to its ability of determining small changes in refractive index at a metal-dielectric interface. The conventional SPR sensor structures are based on Kretschmann's attenuated total reflection (ATR) configuration [5]. In this configuration (fig. 1), a thin metal film is deposited on the surface of a light-coupling substrate and the incident light of wavelength λ excites a p-polarized charge density wave, known as surface plasmon wave (SPW), along the metal surface. Although SPW travels parallel to the metal surface, it also extends evanescently into the adjacent dielectric media. As soon as the propagation constants of SPW and an evanescent wave (generated due to ATR of the incident light) match, a sharp dip in reflected light intensity is observed. If ε_{mr} is the real part of the metal film dielectric function (ε_m), n_c is the refractive index of substrate, and n_s is the refractive index of sensing medium, the resonance condition is given by the following expression:

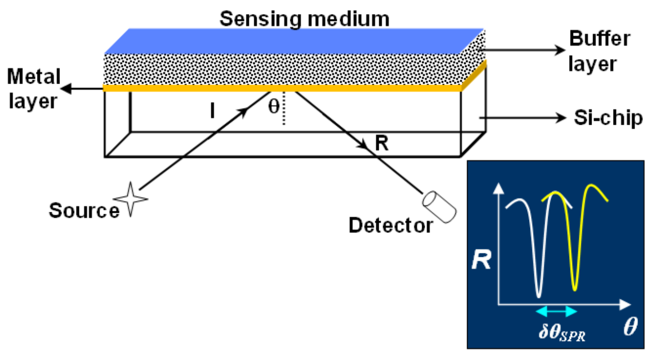

Fig. 1: (Colour on-line) Schematic setup for the SPR-based sensing with silicon substrate.

$$K_0 n_c \sin\theta_{SPR} = K_0\left(\frac{\varepsilon_{mr} n_s^2}{\varepsilon_{mr}+n_s^2}\right)^{1/2}; \quad K_0=\frac{2\pi}{\lambda}. \qquad (1)$$

In eq. (1), θ_{SPR} is known as resonance angle at which SPR dip is observed. The expression on the left side of eq. (1) is the propagation constant (K_{ev}) of the evanescent wave. The right-side expression is the propagation constant (K_{SPW}) of SPW.

(a) Both authors have made equal contribution and should be regarded as first authors of this article.
(b) Currently at: Physics Department, I.I.T. Bhuvaneshwar - India; E-mail: rajaniitd@gmail.com
(c) Currently at: ASML Netherlands B. V. - Veldhoven, The Netherlands; E-mail: anujsharma@gmail.com

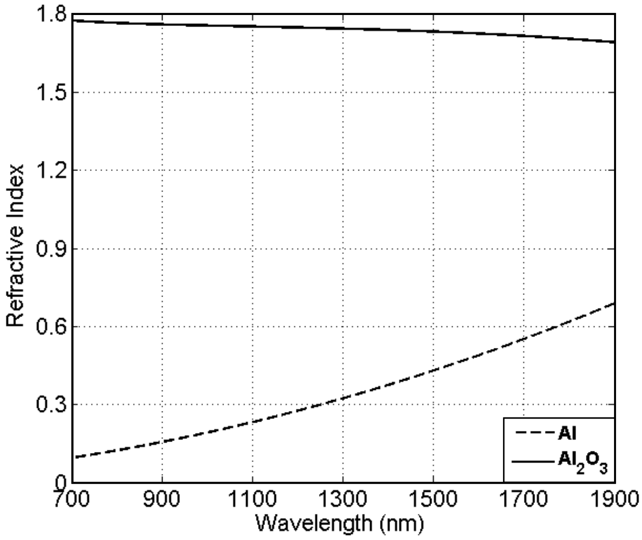

Fig. 2: Refractive index variation of Al and Al_2O_3 in the infrared wavelength region.

Generally, SPR measurements with silica-based substrate do not allow the detection in the infrared (IR) wavelength region, which requires attention due to its many environmental, medical and security applications. Moreover, SPR-based structures in IR have substantially different parameters of excitation and support certain advantages for sensing applications in terms of high probe depth [6] and more accurate determination of the SPR dip [7]. Using a silicon prism for sensing in IR has shown promising results for further studies in this regime [8]. Furthermore, silicon is transparent in IR, therefore, using silicon as a coupling device is very useful from its optical performance viewpoint. More importantly, due to advancements in the micro-nanofabrication technology, one can design a sensor-on-the-silicon-chip for the detection of different physical, chemical and biological parameters [9].

In most of the SPR sensing applications, the metallic layer consists of either silver (Ag) or gold (Au). The Au-based SPR sensor demonstrates a higher angular shift (thus, providing higher detection sensitivity) and is chemically stable against oxidation when operated in liquid and gaseous environments. The Ag-based SPR sensor, on the other hand, displays a narrower resonance curve (thus, providing higher detection accuracy due to smaller errors in the detection of the resonance angle) but is prone to oxidation. In the past, Al has also been used as an SPR-active metal for sensing studies [10]. It has been demonstrated that the Al-based SPR sensor design is able to provide much higher detection accuracy than both Ag- and Au-based designs [11]. However, Al also has poor chemical stability and a thin oxide-layer (*i.e.*, Al_2O_3) covers the Al layer as soon as exposed to air or liquid media. The refractive index of Al_2O_3 differs to that of Al by a large margin (fig. 2), which makes it difficult to get a reliable sensing performance from an Al-based SPR sensor. Thus, the Al layer should be covered with a material, which is compatible in terms of plasmon excitation as well as able to overcome the oxidation problem of Al. Similar to Al, Au being a noble metal fulfills the requirements of being an SPR active medium and can also be capable of overcoming the oxidation problem associated with Al if a bimetallic structure (few nm of Au as outer layer) is used. Therefore, an Al-Au bimetallic combination can be used for designing a SPR sensor, which may not only combine the high detection accuracy of Al and high detection sensitivity of Au, but also address the stability issue.

In the present paper, we have proposed and theoretically analyzed the design of an Al-Au bimetallic-structure–based SPR sensor with silicon substrate in a broad IR region. The single sensor design is shown to be suitable for aqueous as well as gaseous sensing. The sensor's performance has been analyzed in terms of intrinsic sensitivity (IS) that takes into account the shift in the resonance angle, the FWHM of the SPR curve and the refractive index difference of the sensing media. The oxidation problem has been addressed by coating the main Al layer with an ultra-thin Au layer. The physical explanation related to the results has been provided.

Design considerations. – For the present structure, the surface of the silicon substrate is coated with a metal (Al-Au) layer followed by a buffer layer as shown in fig. 1. This buffer layer is finally covered by the sensing medium under detection. The light from the source at a particular wavelength (λ) is launched and the modulated (reflected) light is detected. The dispersion characteristics of all the concerned media (*i.e.*, substrate, the two metals, buffer, and sensing medium) have been taken into account to study the sensor's performance. The refractive index of silicon is wavelength-dependent in the IR region [12,13]. Further, for the dispersion in metal layers, we use the Drude equation as

$$\varepsilon_m(\lambda) = \varepsilon_{mr} + i\varepsilon_{mi} = 1 - \frac{\lambda^2 \lambda_c}{\lambda_p^2(\lambda_c + i\lambda)}, \tag{2}$$

where λ_p and λ_c denote the plasma wavelength and collision wavelength, respectively. The following values of the plasma wavelength and collision wavelength for Au and Al are used: for Au, $\lambda_p = 1.6826 \times 10^{-7}$ m and $\lambda_c = 8.9342 \times 10^{-6}$ m; for Al, $\lambda_p = 1.0657 \times 10^{-7}$ m and $\lambda_c = 2.4511 \times 10^{-6}$ m [11]. For the experimental realization, these thin metal layers can be deposited on the substrate using thermal vapor deposition or the e-beam technique under different optimized conditions [4]. The buffer layer is assumed to be a homogeneous layer of refractive index 1.45. The reason behind taking a buffer layer is twofold. First, it is a well-established fact that taking different substrate materials significantly affects the performance of an optical SPR sensor [14]. In most of the previous studies, the substrate is taken to be made of silica, which has a refractive index in the vicinity of 1.45 and causes SPR excitation mostly in the visible wavelength region. However, the present study considers silicon as the substrate material, which has a refractive index in the vicinity of 3.4 (much higher than that of silica) causing SPR excitation in the infrared region. Therefore, due to a large difference between the refractive indices of substrate (*i.e.*, ~ 3.4) and sensing medium (*i.e.*, ~ 1–1.4), a suitable buffer layer is needed as an intermediate optical medium to achieve an efficient coupling of the incoming light with the plasmon-active area. Second, a suitable buffer layer may keep the gaseous (*i.e.*, lower refractive indices) and biological (*i.e.*, higher refractive indices) samples from being in direct contact of the metal layer, thus, preserving the sensor's detection accuracy against the contamination issues. One such buffer layer can be made of polyethyleneglycol or other similar compounds. The thickness of the buffer layer can be varied from 0 to 150 nm according to the application [15]. For the present study, the buffer layer is assumed to be 25 nm thick. To obtain the expression for the reflected light intensity (R) for p-polarized incident beam, we consider the multilayer transfer matrix method [11].

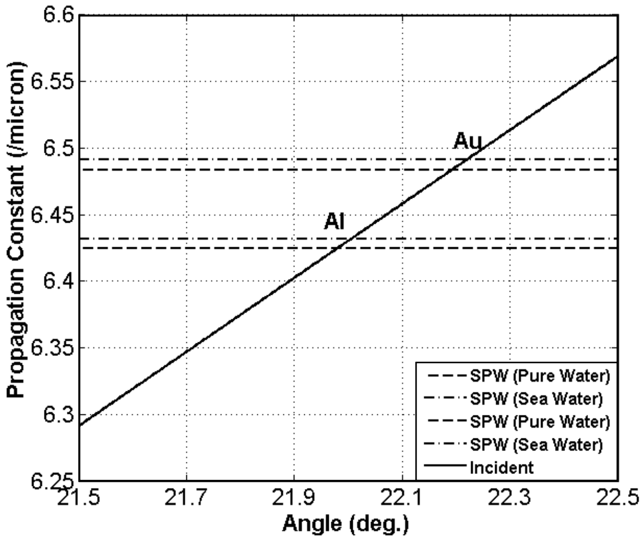

Fig. 3: Illustration of matching of plasmon resonance condition in case of Si substrate for Al and Au layer at two different n_s values.

In general, the performance of SPR sensor is determined in terms of two aspects. First, the shift in resonance angle ($\delta\theta_{SPR}$) for a given change (δn_s) in the sensing-layer refractive index (n_s) should be as large as possible. Second, the full width at half-maximum (FWHM) corresponding to the SPR curves should be as small as possible so that the error in determining the resonance angle is minimum. In order to take both the above aspects into account, a performance parameter called intrinsic sensitivity (IS) is defined as directly proportional to $\delta\theta_{SPR}$ and inversely proportional to the average FWHM of two SPR curves for a given change (δn_s) in the sensing-layer refractive index [7]. Mathematically, the intrinsic sensitivity of the sensor is

$$\mathrm{IS} = \frac{\delta\theta_{SPR}}{\mathrm{FWHM} \times \delta n_s} \qquad (3)$$

Results and discussion. – Three main issues have to be addressed in the context of the present sensor scheme. First, deciding the thicknesses of Al and Au layers in the bimetallic combination. Second, checking the feasibility of the sensor design in a broad range of infrared wavelengths. Third, analyzing the possibility of detecting a broad range of refractive index values with single sensor probe. In the following sections, we sequentially explain the results corresponding to the above-mentioned issues.

Selection of thickness of the Al and Au layers in the bimetallic structure. In a bimetallic-layers–based SPR sensor, the foremost objective is to decide the thickness of the individual metal layers in order to obtain the best possible sensing performance. For this purpose, it is important to analyze how the single Al and Au layers would separately perform as a SPR-active metal in the sensing process, which can be gauged by separately observing the fulfillment of their corresponding resonance conditions (eq. (1)). Figure 3 depicts the separate graphical representations of plasmon resonance condition (eq. (1)) for Au and Al. The angular variations of the propagation constant of the evanescent wave (K_{ev}) for the Si substrate along with those of K_{SPW} for Au and Al are shown. The wavelength of incident light is taken as 1300 nm. The intersection of the curves corresponding to K_{ev} and K_{SP} represents the fulfillment of eq. (1). The two sensing media considered for fig. 3 are pure water and sea water (*i.e.*, pure water with 5% salinity) in terms of the corresponding variation of n_s as described by Scheibener *et al.* [16]. As is visible that for a same value of n_s, there are two different θ_{SPR} values (one each for Al and Au). It confirms that the light coupling as well as plasmon resonance is, in principle, possible by using the Si substrate with either Al or Au as SPR-active metal. Figure 3 also shows that for the same n_s, the resonance takes place at a smaller angle value (θ_{SPR}) for Al than in comparison for Au. However, the shift in the resonance angle ($\delta\theta_{SPR}$) corresponding to an equal change in the refractive index (δn_s) is almost identical for both Al and Au, which is due to the high refractive index of the Si substrate. Figure 4 shows SPR curves for the Al- and Au-based SPR sensor under the conditions mentioned above (*i.e.*, $\lambda = 1300$ nm and the two sensing media being pure water and sea water). The thickness of the Au- and Al-layer is taken as 50 nm. As is clearly visible, the SPR curves corresponding to the Al-based sensor are much sharper than those corresponding to the Au-based sensor. More specifically, the average FWHMs of the SPR curve for Au and Al, respectively, are 0.27° and $0.018°$. The much smaller FWHM for Al can be attributed to the smaller value of the modulus of $\varepsilon_{mr}/\varepsilon_{mi}$ at a given wavelength as compared to Au, where ε_{mr} and ε_{mi} are,

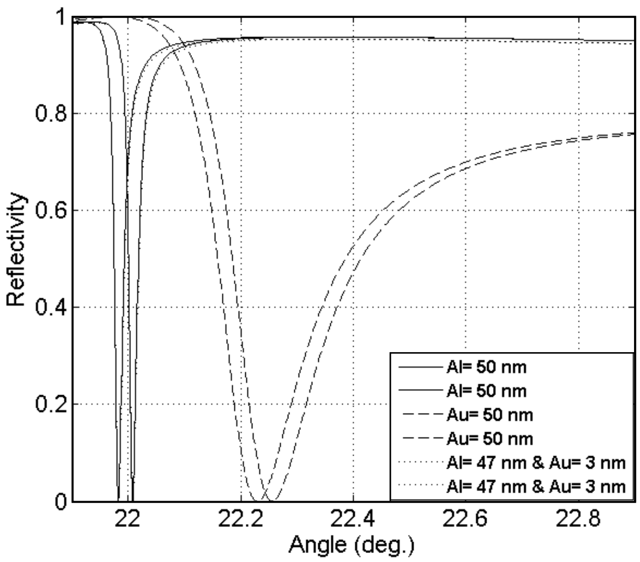

Fig. 4: SPR spectra based on Si substrate for monolayer of Al (50 nm), Au (50 nm) and bimetallic layer (47 nm Al and 3 nm Au) at the operating wavelength of 1300 nm.

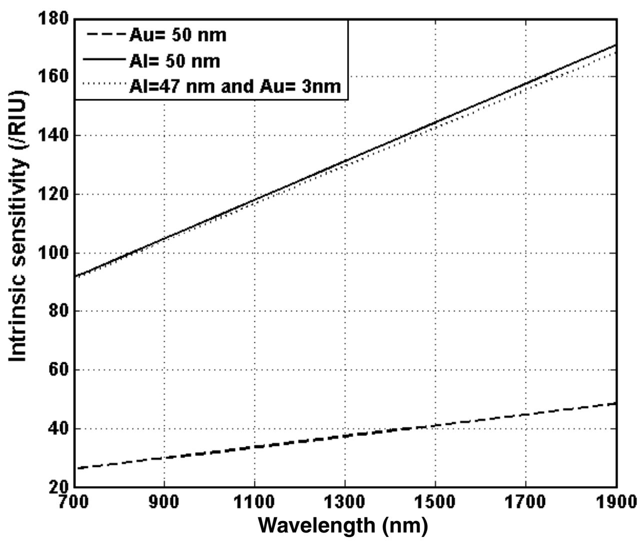

Fig. 5: Variation of the intrinsic sensitivity (IS) with the wavelength of incident light for different cases for aqueous medium.

respectively, the real and imaginary parts of the metal dielectric constant (ε_m). As was clear from fig. 3 also, the shift ($\delta\theta_{SPR}$) in the SPR curve for Au as well as for Al remains the same ($\sim 0.025°$). More precisely, θ_{SPR} shifts from 22.230° to 22.256° in case of Au whereas for Al, the θ_{SPR} shifts from 21983° to 22.008°. Therefore, in view of the above observation that Al and Au have comparable values of $\delta\theta_{SPR}$, Al has a clear edge over Au due to its much smaller FWHM. Therefore, it will be useful to design a SPR sensor with Al as main metal layer coated with an ultra-thin Au layer. For instance, a 47 nm thick Al layer coated with a 3 nm thick Au layer. Figure 4 also contains the SPR curve for a bimetallic case with 47 nm thick Al (inner) layer and 3 nm thick (outer) Au layer. The above curve is so close to that corresponding to the Al (50 nm) curve that the two curves are almost merged together. The angular shift ($\delta\theta_{SPR}$) and the FWHM of the SPR curve remains almost same as in case of a sensor with 50 nm thick Al. Hence, the performance of a SPR sensor with the proposed bimetallic combination remains very close to the Al monolayer case. Moreover, the Au layer protects the Al layer from getting oxidized. It is worth mentioning here that the Al layer does not form any alloy with the 3 nm thick Au layer. However, for higher thickness (> 15 nm), the possibility of alloy formation may exist under different conditions [17]. Another study [18] has shown that the estimated thickness of the surface oxide layer on Al film is $\sim$2–3 nm and therefore a 3 nm Au layer must principally protect the thicker Al layer against oxidation.

Analysis of design parameters in infrared sensing. After deciding the thickness combination of the Al-Au bimetallic structure, the next task is to analyze the feasibility of the proposed sensor scheme in a broad IR wavelength range. For this purpose, we study the effect of incident wavelength on the sensor's performance parameter, *i.e.*, intrinsic sensitivity (as defined in eq. (3)). Figure 5 shows the variation of intrinsic sensitivity with incident wavelength for three different cases, *i.e.*, Al (47 nm)-Au (3 nm) bimetallic structure, Al (50 nm) monolayer, and Au (50 nm) monolayer. The figure corresponds to liquid sensing with pure water and sea water as the two sensing media. The incident wavelength has been varied from 700 nm to 1900 nm, which covers a large range (1200 nm) of IR wavelengths. It can be observed that under the same design conditions over a broad wavelength band in the IR region, the intrinsic sensitivity is almost 350% higher when the Al layer is used as compared to the sensor based on the Au layer. It can also be noted that the oxidation problem of the Al-based sensor can be easily handled by using 3 nm of Au layer which lowers the intrinsic sensitivity of the sensor by around 2 to 3%, which is negligible considering the fact that a thin layer of Au enhances the longevity of the sensor. The increase in intrinsic sensitivity with increasing wavelength can be explained in terms of the imaginary part of K_{SPW} (that corresponds to the optical absorption of incident light), which has an inverse variation with wavelength. So, this inverse spectral dependence of the optical absorption implies that light absorption increases with a decrease in wavelength which causes the reflected-light intensity (R) to decrease and the SPR curve shifts downward. Thus, the shorter the wavelength the greater the downward shifting (*i.e.*, broadening) of the SPR curve. Further, the angular shift of the SPR dip also gets affected by the wavelength because of the corresponding dependences of the real part of the metal dielectric constant

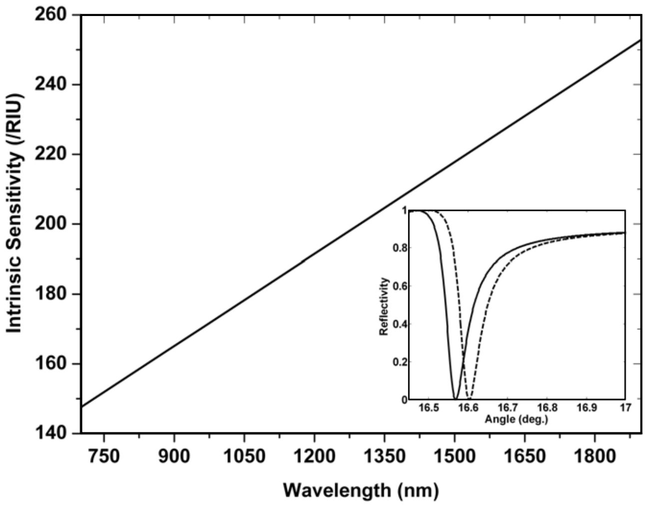

Fig. 6: Variation of the intrinsic sensitivity (IS) with the wavelength of incident light for different cases for gaseous medium. The inset shows the SPR curves for Si-based sensors at 1300 nm with Al-Au bimetal.

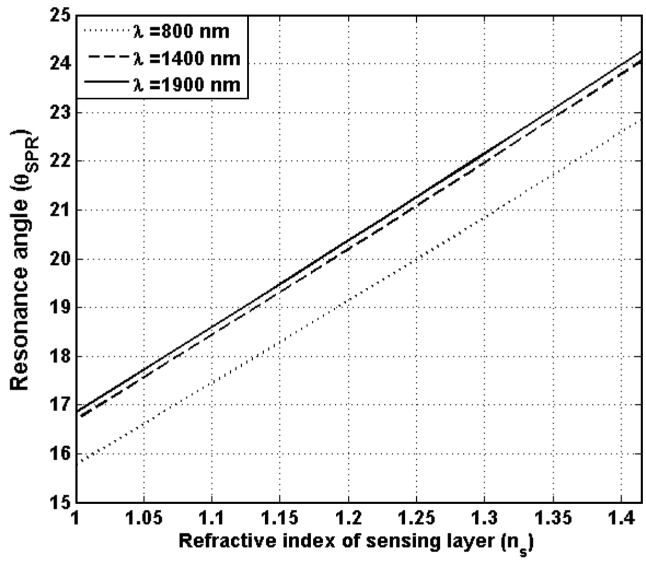

Fig. 7: Variation of the resonance angle (θ_{SPR}) for a range of sensing medium refractive index (n_s) 1.001–1.417 RIU. The variation is plotted for three different infrared wavelengths.

and hence the real part of K_{SPW}. However, the influence of the wavelength is more prominent on the imaginary part rather than the real part of K_{SPW}. Therefore, the variation of IS with wavelength is largely dictated by the SPR curve's FWHM in comparison to its shifting. Since the FWHM of the SPR curve is greater at shorter wavelength, therefore, IS gets better at higher wavelength. This suggests that sensor's performance gets better as one operates with far-IR wavelengths, depending on the specific requirement of the concerned application.

Liquid and gas sensing with single-sensor design. Due to crucial environmental concerns, there is a serious requirement of precise sensors in the IR region for the detection of various gases. The present state of the art suggests that SPR sensors are largely unexplored for gas sensing in the IR wavelength range. In this view, we further extended our proposed sensor scheme based on the Si substrate and the Al (47 nm)-Au (3 nm) bimetal for gas detection in the infrared regime. Figure 6 shows the variation of IS with the wavelength of incident light in the range from 700 to 1900 nm. The inset in the same figure shows the SPR curves corresponding to the Si substrate at an incident wavelength of 1300 nm for gaseous refractive indices 1.001 and 1.003 (*i.e.*, $\delta n_s = 0.002$ RIU). In the inset figure, the value of $\delta\theta_{SPR}$ is 0.035° (*i.e.*, θ_{SPR} changes from 16.568° to 16.603°) for the Si-based gas sensor, whereas the average FWHM of the SPR curve is 0.072°. The main figure also shows a similar trend of increase in intrinsic sensitivity with wavelength. The higher intrinsic sensitivity is mainly due to relatively smaller FWHM as explained in last section for liquid sensing. It implies that the present sensor scheme is applicable for gas sensing as well. Figure 7 shows the calibration curve for the present sensor scheme covering a large range of n_s values from 1.001 RIU (*i.e.*, beginning of gaseous medium) to 1.417 RIU (*i.e.*, high-index liquid medium) at three different IR wavelengths. The resonance angle (θ_{SPR}) values are comfortably in the measurable range at any incident wavelength. This clearly indicates that the present sensor scheme with Si-substrate and Al-Au bimetal is able to detect both gaseous and liquid media with a single-sensor probe.

Conclusion. – A high-performance SPR sensor based on silicon substrate and Al-Au bimetallic layers is proposed. With Si-substrates, it can be easily possible to design miniaturized and compact SPR sensor chips due to already existing nano-micro fabrication advancements. Such unique advantage of compact sensor chips is not possible with the bulk glass materials such as silica and chalcogenide. Further, as the results indicate, it is possible to cover a much larger range of sensing media with an Si substrate due to its much higher refractive index than the above bulk glass materials. So, our proposed single Si-based SPR probe in its miniaturized form can enable the detection of gaseous, liquid, and biological media with high sensitivity, precision, and stability. Furthermore, the performance of the proposed sensor gets better at higher wavelengths, which makes it especially useful in the infrared wavelength region.

A few possible first-hand applications may be such as environmental analysis, breath-analysis, homeland security, and minerals detection. We believe that the proposed model can open a new route in the sensing research for silicon-based miniaturized plasmonic sensors by riding on the advantages of the latest micro-nanofabrication techniques to design lab-on-a-chip for the detection of different physical, chemical and biological parameters.

* * *

We are grateful to all our colleagues for several positive discussions and suggestions.

REFERENCES

[1] Liedberg B. *et al.*, *Sens. Actuators*, **4** (1983) 299.
[2] Wang T. J. *et al.*, *Photonics Technol. Lett.*, **16** (2004) 1715.
[3] Haes A. J. *et al.*, *Nano Lett.*, **4** (2004) 1029.
[4] Rajan *et al.*, *Sens. Actuators B*, **123** (2007) 661.
[5] Kretschmann E. and Reather H., *Z. Naturforsch.*, **23** (1968) 2135.
[6] Nelson B. P. *et al.*, *Anal. Chem.*, **71** (1999) 3928.
[7] Johansen K. *et al.*, *Rev. Sci. Instrum.*, **71** (2000) 3530.
[8] Patskovsky S. *et al.*, *Sens. Actuators B*, **97** (2004) 409.
[9] Wang X *et al.*, *Appl. Phys. Lett.*, **92** (2008) 013903.
[10] Krane K. J. and Reather H., *Phys. Rev. Lett.*, **37** (1976) 1355.
[11] Sharma A. K. and Gupta B. D., *J. Appl. Phys.*, **101** (2007) 093111.
[12] Adachi S., *Phys. Rev. B*, **38** (1988) 12966.
[13] Tatian B., *Appl. Opt.*, **23** (1984) 4477.
[14] Gupta G. and Kundoh J., *Sens. Actuators B*, **122** (2007) 381.
[15] Sharma A. K. and Gupta B. D., *Sens. Actuators B*, **107** (2005) 40.
[16] Scheibener P. *et al.*, *J. Phys. Chem. Ref. Data*, **19** (1990) 677.
[17] Mcintyre N. S. *et al.*, *Appl. Surf. Sci.*, **144** (1999) 156.
[18] Mitsushio *et al.*, *Sens. Actuators A*, **125** (2006) 296.